Journal of
Materials Chemistry C

Accepted Manuscript

This article can be cited before page numbers have been issued, to do this please use: J. Yang, N. Sun, J. Huang, Q. Li, Q. Peng, X. Zhang, Y. Q. Dong, D. Ma and Z. Li, *J. Mater. Chem. C*, 2015, DOI:

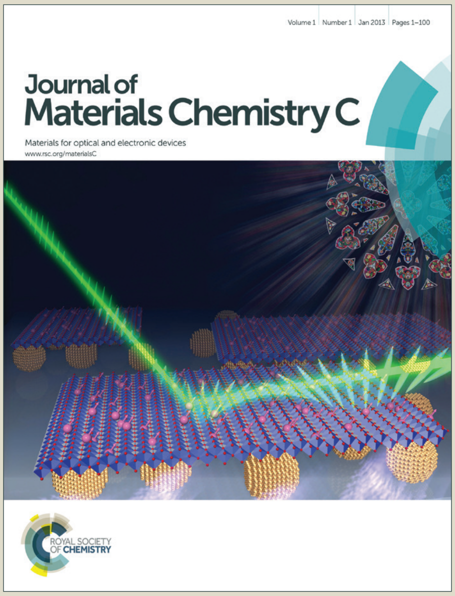

ROYAL SOCIETY
OF CHEMISTRY

www.rsc.org/materialsC

View Article Online
DOI: 10.1039/C4TC02631D

Journal Name

RSCPublishing

ARTICLE

Cite this: DOI: 10.1039/x0xx00000x

Received 00th January 2012,
Accepted 00th January 2012

DOI: 10.1039/x0xx00000x

www.rsc.org/

New AIEgens containing tetraphenylethene and silole moieties: tunable intramolecular conjugation, aggregation-induced emission characteristics, and good device performance†

Jie Yang,[a] Ning Sun,[b] Jing Huang,[a] Qianqian Li,[a] Qian Peng,[c] Xi Tang,[d] Yongqiang Dong,[d] Dongge Ma*[b] and Zhen Li*[a]

Three aggregation-induced emission (AIE) luminogens (Si-*p*TPE, Si-tPE and Si-*m*TPE) were successfully obtained by the covalent incorporation of tetraphenylethene to dibenzosilole core. Through sharing benzene ring and changing link mode between TPE and silole core, their emission colours were tuned from green to sky blue even deep blue. The non-doped OLED device based on Si-tPE exhibits sky blue light with high luminance (up to 27161 cd m^{-2}) and high current, power and external quantum efficiencies (up to 8.04 cd A^{-1}, 6.17 lm W^{-1} and 3.38%, respectively).

Introduction

Recently, AIEgens, one special kind of luminogens exhibiting weak luminescence in solutions but much, even dramatically enhanced emission in aggregation state, such as solid state or nanoparticles, have attracted increasing attention, due to their totally different emissive behaviour against the notorious aggregation-caused quenching (ACQ) effect and huge potential applications as light emitting diodes (LED), chemo- and bio-sensors, fluorescent patterns, *et al.*, since their first report in 2001 by the group of Ben Zhong Tang.[1] As a typical example, 1-methyl-1,2,3,4,5-pentaphenylsilole (MPPS, one famous molecule of the silole family, Figure 1), with a highly twisted structure, demonstrated a very high efficiency of 8% when acting as the emissive layer in the corresponding LED device, which approached the theoretical limitation of the OLEDs based on fluorescent luminogens.[2] Stimulated by this exciting result, many efficient AIEgens have been designed and showed satisfactory performance in their related LED devices, for example, once bulky dimesitylboryl, 9,9-dimethylfluorenyl, 9,9-diphenylfluorenyl, and 9,9-spirobifluorenyl substituents were introduced into the 2,5-positions of silole rings, the resulted AIEgens all exhibited outstanding EL performance, even up to 16.0 cd A^{-1}.[3] However, it was a little pity that similar to other fluorescent luminogens, there were few reports concerning the blue AIE fluorophors, once again showing the difficulty to achieve good blue organic light-emitting materials, derived from their intrinsic wide band gap.[4] Interestingly, once incorporating TPE moieties, another famous AIE construction block with inherent blue emission to MPPS core, the resultant 2,5-BTPEMTPS (Figure 1), also possessed relatively good performance (6.4 cd A^{-1}), with the electroluminescence emission peak of 552 nm, longer than that of MPPS, as the result of the prolonged conjugation length.[5]

Recently, by simply sharing benzene ring, utilizing different linkage modes, and increasing the twisting degree of the molecules in the presence of additional groups, we have successfully constructed some blue AIEgens, which exhibited good performance as emitting layer in OLEDs, partially due to their AIE characteristics.[6] Thus, is it possible to apply these strategies to the above mentioned TPE-silole system, to develop some new AIEgens with blue emissions, but not the green one as 2,5-BTPEMTPS?

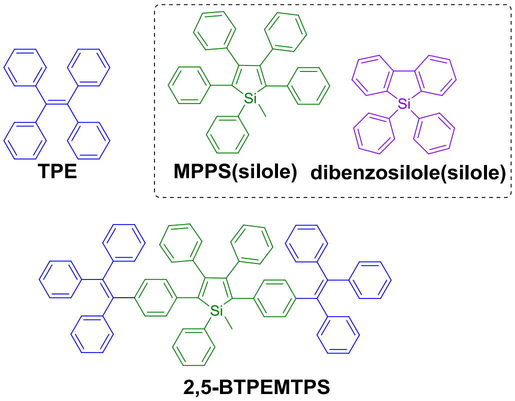

Figure 1. Chemical structures of TPE, MPPS, dibenzosilole and 2,5-BTPEMTPS.

View Article Online
DOI: 10.1039/C4TC02631D

Journal Name

RSCPublishing

ARTICLE

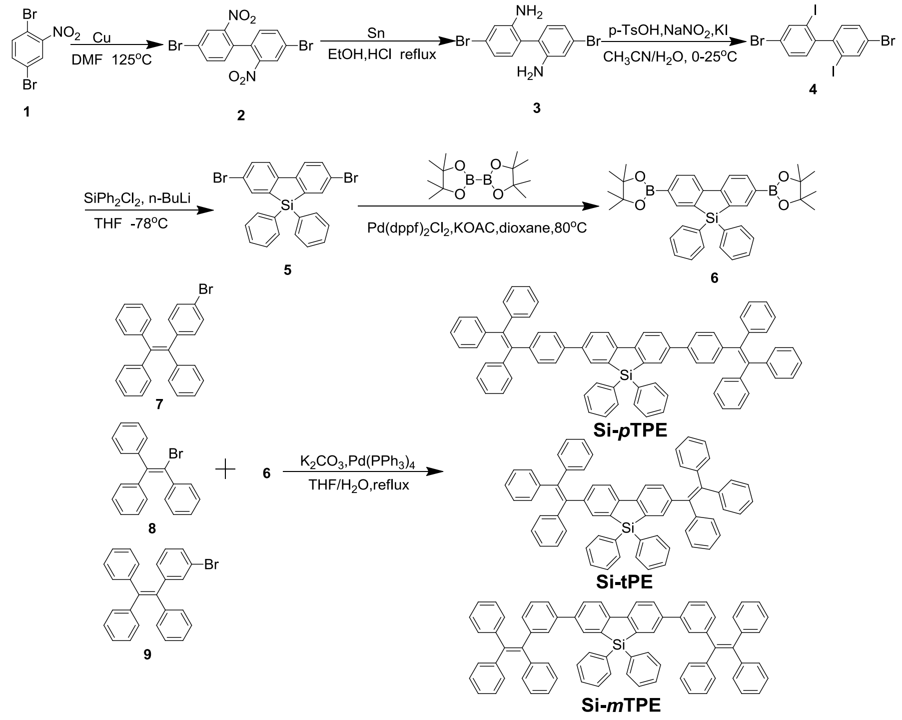

Scheme 1. Synthetic route to Si-*p*TPE, Si-tPE and Si-*m*TPE.

To control the conjugation length and simplify the synthesis, in addition to the above mentioned strategies, we utilized another silole-derivative, dibenzosilole, instead of MPPS, as the construction block, and incorporated TPE moieties to yield three AIEgens (Si-*p*TPE, Si-tPE and Si-*m*TPE), in which the approaches of *para*-position linkage, sharing benzene ring and *meta*-position linkage between silole and TPE groups, were applied respectively. The results partially confirmed our idea. The OLED devices based on these AIEgens exhibit green, sky blue and deep blue emission, respectively. Among them, Si-tPE shows the best performance of 8.04 cd A^{-1} with sky blue emission. Herein, we would like to present the syntheses, characterization, photophysical properties, theoretical calculation and LED device performance of these AIEgens in detail.

Results and discussion

Synthesis

Scheme **1** shows the synthetic route to Si-*p*TPE, Si-tPE and Si-*m*TPE, and the detailed procedures are presented in the experimental section.[7] First, we prepared compound **2** through Ullmann reaction under the catalyst of copper powder in a high yield, then nitro-groups were reduced to yield compound **3**. The amidogen of compound **3** was replaced by iodine, and the key intermediate, compound **5**, was synthesized through ring-closing reaction between compound **4** and dichlorodiphenylsilane. The corresponding diboronic ester for compound **5** was successfully obtained in a good yield using Pd(dppf)$_2$Cl$_2$ as the catalyst. Compound **7**, **8** and **9** were synthesized according to the literatures.[6,8] Finally, the desired products of Si-*p*TPE, Si-tPE and Si-*m*TPE were successfully afforded through the Suzuki cross-coupling reactions and they were all purified by column chromatography on silica gel using petroleum ether and chloroform as eluent, and fully characterized by ^{1}H and ^{13}C NMR, mass spectrometry, and elemental analysis (Figure S1- S10).

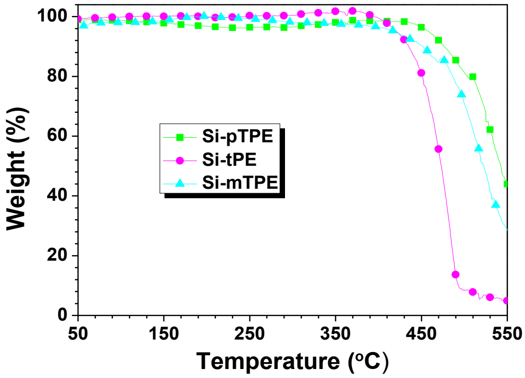

Figure 2. TGA thermograms of Si-*p*TPE, Si-tPE and Si-*m*TPE recorded under N_2 at a heating rate of 10 °C/min.

Table 1. The thermal, electrochemical and photophysical data of Si-*p*TPE, Si-tPE and Si-*m*TPE.

	T_d[a] (°C)	T_g (°C)	E_g[b] (eV)	E_{ox} (V)	E_{HOMO}[c] (eV)	E_{LUMO}[d] (eV)	λ_{abs}[e] (nm)	ε[f] ($\times 10^4$ M^{-1} cm^{-1})	PL λ_{max} (aggr)[g] (nm)	PL λ_{max} (film) (nm)
Si-*p*TPE	458	196	3.02	1.15	5.47	2.45	359	5.87□	498	498
Si-tPE	421	107	2.99	1.08	5.40	2.41	362	3.31	498	496
Si-*m*TPE	411	---	3.32	1.27	5.60	2.28	325	7.45	474	468

[a] 5% weight loss temperature measured by TGA under N_2. [b] Band gap estimated from optical absorption band edge of the solution. [c] Calculated from the onset oxidation potentials of the compounds. [d] Estimated using empirical equations $E_{LUMO} = E_{HOMO} + E_g$. [e] Observed from absorption spectra in dilute THF solution. [f] Molar extinction coefficient. [g] Determined in THF:H_2O = 1:99 solution.

Thermal properties

We carried out TGA (thermo gravimetric analysis) and DSC (differential scanning calorimetry) to examine their thermal properties. As shown in Figure 2, they were all thermally stable, with their thermal-decomposition temperatures (T_d, corresponding to 5% weight loss) higher than 410 °C. Also, Si-*p*TPE and Si-tPE exhibited relatively high glass transition temperatures (T_g), namely 196 and 107 °C, respectively (Table 1, Figure S11). Unfortunately, the DSC curve of Si-*m*TPE showed no obviously T_g. Thus, the good thermal stability with high T_d and T_g values would contribute to the long lifetime, when they were made into OLED devices.[9]

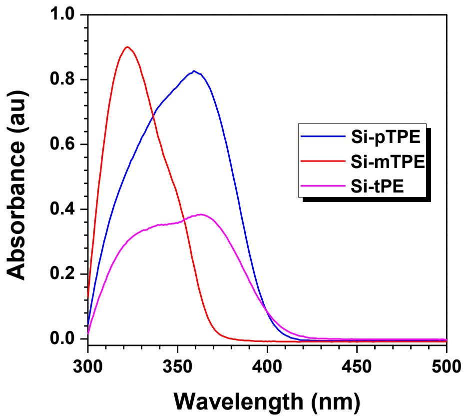

Figure 3. UV spectra in THF solution. Concentration (μM): 14.1, 11.6 and 12.1 for Si-*p*TPE, Si-tPE and Si-*m*TPE, respectively.

AIE properties and theoretical calculations

In the UV-vis spectra of Si-*p*TPE, Si-tPE and Si-*m*TPE recorded in THF solution (Figure 3), their maximum absorption peaks located at 359, 362 and 325 nm respectively. The results indicated that Si-*m*TPE exhibited the weakest conjugation, while Si-*p*TPE and Si-tPE were almost the same. In comparison with that of 2,5-BTPEMTPS (395 nm), all these three compounds possessed much blue-shifted, as the result of their controlled intramolecular conjugation effect. Analyzing the absorption behaviours of Si-*p*TPE and Si-*m*TPE carefully, although the ignorable difference was the linkage mode between the TPE moieties and dibenzosilole, there was a big difference, as large as 34 nm, in their maximum absorption wavelength. This confirmed again the powerful control of intramolecular conjugation by simply changing the linkage mode, realizing our design idea.

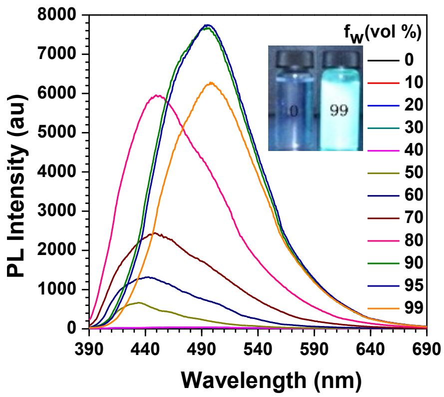

Figure 4. (A) PL spectra of Si-*p*TPE in THF–H_2O mixtures with different water fractions. Concentration (μM): 14.1; excitation wavelength (nm): 370.

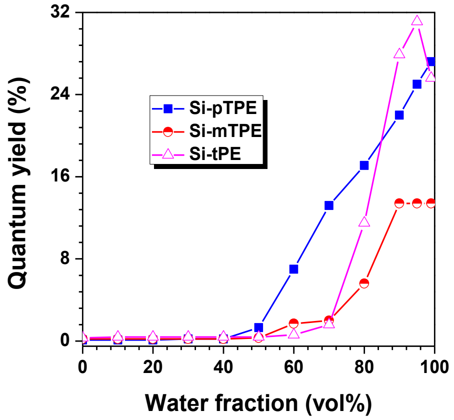

Figure 5. Plots of fluorescence quantum yields of Si-*p*TPE, Si-tPE and Si-*m*TPE determined in THF/H_2O solutions by using 9,10-diphenylanthracene (Φ = 90% in cyclohexane) as standard *versus* water fractions.

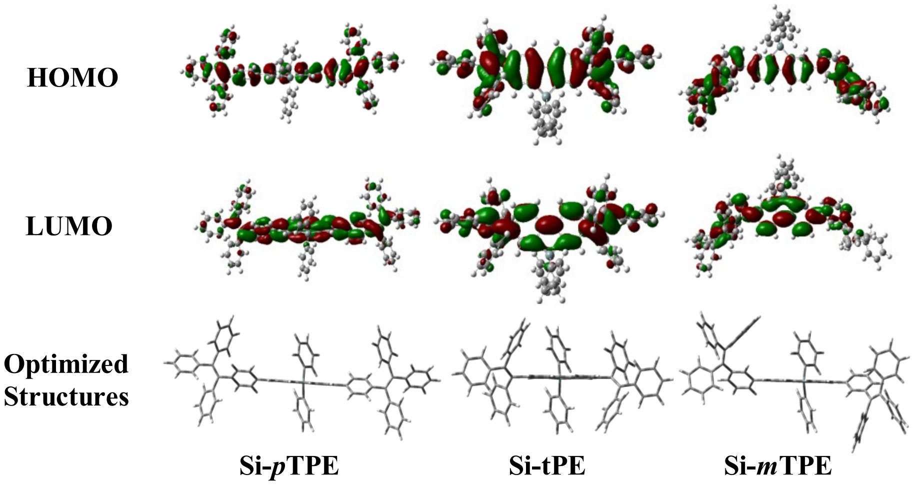

Figure 6. Calculated molecular orbital amplitude plots of LUMO, HOMO levels and optimized molecular structures for Si-*p*TPE, Si-tPE and Si-*m*TPE.

In order to investigate the possible AIE characteristics of these three molecules, their fluorescent behaviours were studied. We chose tetrahydrofuran as the good solvent while water as the poor one. As shown in Figure 4 and Figure S12，Si-*p*TPE, Si-tPE and Si-*m*TPE were all nonemissive in pure THF, however, after a large amount of water was added, they all emitted strong fluorescence. Figure 5 demonstrated the changes of their fluorescence quantum yield (Φ_F) in THF/water mixtures with different water fractions (f_w), which enabled fine-tuning of the solvent polarity and the extent of solute aggregation. In pure THF solution, they were all less than 0.3%, while at a f_w value of 99%, the Φ_F of Si-*p*TPE and Si-tPE exceeded 25%, while that of Si-*m*TPE was limited to 13%, only about half to its analogue, possibly due to their different molecular structures. Anyhow, these three luminogens are all AIE-active.

Although their crystal structures were not obtained, the calculated ones could still give some explanations. The geometries of the molecules have been optimized by using DFT calculations with the Gaussian 09 program. In particular, we used the B3LYP exchange-correlation functional and a 6-31g* basis set. As shown in Figure 6, the structure of Si-*m*TPE was much more twisted than Si-*p*TPE and Si-tPE, which might provide more room for the rotation of the phenyl rings even in aggregation state, thus, much energy would be consumed through the intramolecular rotation, resulting in its lower Φ_F.[6]

Also when we investigated their AIE characteristics, we found the emission of Si-*p*TPE was red-shifted about 80 nm after the addition of excessive water (f_w > 80%), while no obvious change for those of Si-tPE and Si-*m*TPE. This could be explained from the distribution of their different electron clouds. As shown in Figure 6, the molecular orbital amplitude plots of the HOMO and LUMO energy levels for Si-tPE overlapped perfectly, indicating no intramolecular charge transfer (ICT) existed. However, those of Si-*p*TPE and Si-*m*TPE partly overlapped, which might lead to the ICT effect. As to Si-*m*TPE, its molecular structure was much twisted, which would weaken the ICT effect. So, once a large amount of water was added, the polarity of the mixed solvent increased accordingly, as a result, the ICT effect occurred in the case of Si-*p*TPE much easier, directly leading to the red-shifted emission. On the other hand, with addition of water, the transformation from crystalline state to amorphous one would also contribute to it. But as to the cases of Si-tPE and Si-*m*TPE, nearly no influences were observed.

Electrochemical Properties

The electrochemical properties of Si-*p*TPE, Si-tPE and Si-*m*TPE were investigated by cyclic voltammetry (CV) (Figure S13). The HOMO energy levels were calculated to be 5.47, 5.40 and 5.60 eV respectively, according to the following equation: HOMO = - (4.8 - $E_{(Fc/Fc+)}$ + E_{ox}) eV in which $E_{(Fc/Fc+)}$ is 0.48 eV, suggesting that Si-tPE might possess the best hole-injection ability among the three AIEgens. Their LUMOs could be obtained from optical band gap energies (estimated from the onset wavelength of their UV absorptions) as 2.45, 2.41 and 2.28 eV for Si-*p*TPE, Si-tPE and Si-*m*TPE respectively. Thus, Si-*p*TPE and Si-tPE possessed better electronic injection capacity, possibly affecting their performance in OLED devices largely.

Electroluminescence

Due to their good thermal stabilities and efficient light emissions in the solid state, we fabricated their non-doped OLED devices with a configuration of ITO/MoO_3 (10 nm)/NPB (60 nm)/EML (15 nm)/TPBi (30 nm)/LiF (1 nm)/Al. In these OLED devices, MoO_3, NPB worked as the hole-injection, hole transporting layer respectively, and TPBi acted as electron transporting as well as hole

View Article Online
DOI: 10.1039/C4TC02631D

Table 2. EL performance of Si-*p*TPE, Si-tPE and Si-*m*TPE.

	λ_{EL} (nm)	V_{on} (V)	L_{max} (cd m^{-2})	$\eta_{P, max}$ (lm W^{-1})	$\eta_{C, max}$ (cd A^{-1})	$\eta_{ext, max}$ (%)	CIE (x, y)
Si-*p*TPE	512	3.5	28718	5.57	7.40	2.92	0.21, 0.37
Si-tPE	488	3.0	27161	6.17	8.04	3.38	0.20, 0.33
Si-*m*TPE	432	3.7	4411	1.18	1.39	1.21	0.16, 0.12

Abbreviations: V_{on} = turn-on voltage at 1 cd m^{-2}, L_{max} = maximum luminance, $\eta_{P, max}$, $\eta_{C, max}$ and $\eta_{ext, max}$ = maximum power, current and external quantum efficiencies, respectively. CIE = Commission International de l'Eclairage coordinates.

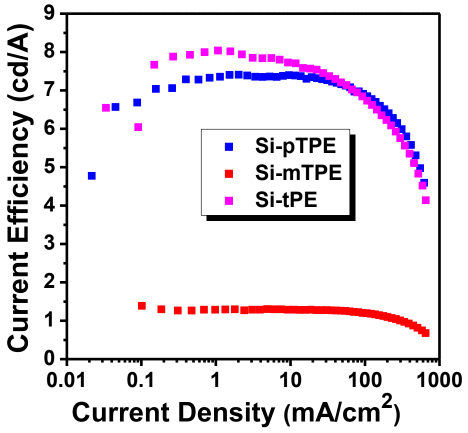

Figure 7. Changes in current efficiency with the current density, Device configuration: ITO/MoO_3 (10 nm)/NPB (60 nm)/Si-*p*TPE or Si-*m*TPE or Si-tPE (15 nm)/TPBi (30 nm)/LiF (1 nm)/Al.

blocking layer. Si-*p*TPE, Si-tPE and Si-*m*TPE served as emitters. Fig 7 and Figure S14 showed the current density-voltage-brightness (*J-V-L*) characteristics, current efficiency, power efficiency and external quantum efficiency *versus* current density curves of the OLEDs. As listed in Table 2, all the devices turned on at a low voltage from 3.0 to 3.7 V, showing small injection barriers from transporting layers in the devices. Among them, Si-tPE exhibited the best performance, with a maximum luminance (L_{max}) of 27161 cd m^{-2}, a maximum current efficiency ($\eta_{C, max}$) of 8.04 cd A^{-1}, a maximum power efficiency ($\eta_{P, max}$) of 6.17 lm W^{-1} and a maximum external quantum efficiency ($\eta_{ext, max}$) of 3.38%. The EL spectrum of the device peaked at 488 nm (sky blue), which was slightly blue-shifted from the PL peaks of the thin film (496 nm) and nanoaggregates (498 nm) of Si-tPE, indicating that the emitting layer partly crystallized (Figure 8).

The device based on Si-*p*TPE also presented a good performance with a maximum current efficiency ($\eta_{C, max}$) of 7.40 cd A^{-1}, but its EL spectrum was red-shifted to 512 nm, which was out of the blue area. So only removing a phenyl ring between the tetraphenylethene group and dibenzosilole core, the EL emission based on Si-tPE was blue-shifted about 24 nm, in comparison with Si-*p*TPE while its current efficiency was higher. The cheerful performance might be owed to the reason that Si-tPE was in a more planar conformation and showed a better carrier mobility, but the length of the conjugation is shorter for a lack of phenyl ring which will contribute to its blue-shift. As for Si-*m*TPE, the device showed an emission centred at 432 nm (deep blue). Compared to its PL spectra of the thin film (468 nm) and nanoaggregates (474 nm), its EL spectrum was blue-shifted more than 35 nm, manifesting the emitting layer mainly existed in crystal.[10] Generally, crystals are a two-edged sword: on one hand, it would be helpful to construct blue materials, but on the other, the LED device based on it will exhibit an inferior performance, since the grain boundaries between adjacent crystallites act as traps for charge carriers.[11] The device based on Si-*m*TPE showed an unsatisfactory performance (1.39 cd A^{-1}) compared to its analogues. Rather than Si-*p*TPE, although the ignorable difference was the linkage mode between the TPE moieties and dibenzosilole for Si-*m*TPE, there was a big difference, as large as 80 nm, in their maximum EL emission. This confirmed the powerful control of intramolecular conjugation by simply changing the linkage mode.

View Article Online
DOI: 10.1039/C4TC02631D

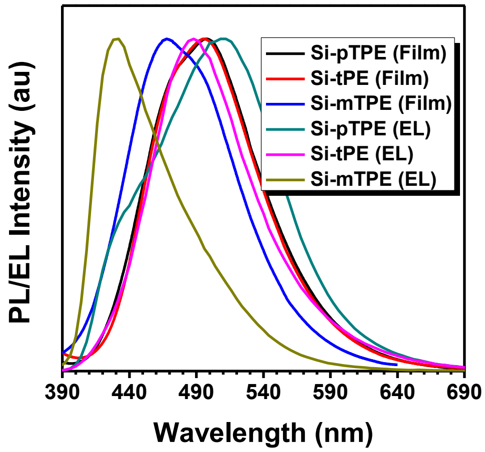

Figure 8. PL and EL spectra of solid thin films of Si-*p*TPE, Si-tPE and Si-*m*TPE. The thin films were spin-coated onto ITO glass from dilute THF solution with concentrations of 1 mg mL^{-1}.

Conclusions

In summary, three AIEgens (Si-*p*TPE, Si-tPE and Si-*m*TPE) based on tetraphenylethene and silole were obtained. These three new compounds were nonemissive in the solution state, but highly emissive when aggregated, showing typical AIE effect. They exhibited high thermal stability and great EL performance. The best performance was achieved for Si-tPE (L_{max} of 27161 cd m^{-2}, $\eta_{C,\,max}$ of 8.04 cd A^{-1}, $\eta_{P,\,max}$ of 6.17 lm W^{-1} and $\eta_{ext,\,max}$ of 3.38% at 488 nm), thanks to the high electron mobility of silole and AIE nature of TPE. Just through small structural modulation of sharing benzene ring and changing link mode between TPE and silole core, their EL spectra were tuned from green to sky blue even deep blue. We may believe that, inspired by these preliminary results, many other AIE luminophores with better performance and blue emission could be further developed.

Experimental section

Characterization

^{1}H and ^{13}C NMR spectra were measured on a Mecuryvx300 spectrometer or Bruker Advance III (400 MHz) spectrometer. Elemental analyses of carbon and hydrogen were measured on a Perkin-Elmer microanalyzer. Mass spectra were measured on a Bruker BIFLEX Ш TOF or JEOL LMS-HX-110 mass spectrophotometer. UV-vis absorption spectra were recorded on a Shimadzu UV-2500 recording spectrophotometer. Photoluminescence spectra were recorded on a Hitachi F-4500 fluorescence spectrophotometer. Differential scanning calorimetry (DSC) was performed on a NETZSCH DSC 200 PC unit at a heating rate of 15 °C min^{-1} from room temperature to 300 °C under argon. Thermogravimetric analysis (TGA) was undertaken with a NETZSCH STA 449C instrument. The thermal stability of the samples under a nitrogen atmosphere was determined by measuring their weight loss while heating at a rate of 10 °C/min from 50 to 550 °C. Cyclic voltammetry (CV) was carried out on a CHI voltammetric analyzer in a three-electrode cell with a Pt counter electrode, a Ag/AgCl reference electrode, and a glassy carbon working electrode at a scan rate of 100 mV s^{-1} with 0.1 M tetrabutylammonium perchlorate (purchased from Alfa Aesar) as the supporting electrolyte, in anhydrous dichloromethane solution purged with nitrogen. The potential values obtained in reference to the Ag/Ag^{+} electrode were converted to values *versus* the saturated calomel electrode (SCE) by means of an internal ferrocenium/ferrocene (Fc^{+}/Fc) standard.

Computational details

The geometrical and electronic properties were optimized at B3LYP/6-31g* level using Gaussian 09 program. The molecular orbitals were obtained at the same level of theory.

OLED device fabrication and measurement

The EL devices were fabricated by vacuum deposition of the materials at a base pressure of 5×10^{-6} torr onto glass pre-coated with a layer of indium tin oxide (ITO) with a sheet resistance of 25 Ω/square. Before the deposition of an organic layer, the clear ITO substrates were treated with oxygen plasma for 3 min. The deposition rate of organic compounds was 0.9-1.1 Å s^{-1}. After the hole-injection layer MoO_3, hole-transporting layer 1,4-bis(1-naphthylphenyl-amino)biphenyl (NPB), emission layer, electron-transporting layer 1,3,5-tris(N-phenyl-benzimidazol-2-yl)benzene (TPBI), and lithium fluoride (LiF) were deposited by the thermal evaporation under a base vacuum of $\sim10^{-6}$ torr, aluminium (Al) metal was evaporated in another vacuum chamber without breaking the vacuum. The *J–V–L* of the devices was measured with a Keithley 2400 Source meter and Keithley 2000 Current meter. The EL spectra were measured by JY SPEX CD3000 fluorescence spectrophotometer and PR650 Spectra Scan Photometer. All measurements were carried out at room temperature under ambient conditions.

Preparation of compounds

Solvents for chemical synthesis were purified according to the standard procedures. Compound **7**, **8** and **9** were synthesized according to the literatures.[6,8] All other chemicals and reagents were obtained from commercial sources and used as received.

Synthesis of compound 2[12]

Compound **1** (14.1 g, 50 mmol) and copper power (7.0 g, 109 mmol) in DMF (55 mL) were added into a 200 mL Schlenk tube, The resultant mixture was stirred for 1 hour under argon at 125 °C. After cooling to room temperature, the brown residue was filtered off and washed with 20 mL of toluene. Then the filtrate was distilled under reduced pressure. The crude product was purified by column chromatography on silica gel using petroleum ether/chloroform (v/v = 4/1) as eluent, a yellow solid was finally obtained in the yield of 91% (9.18 g). ^{1}H NMR (400 MHz, $CDCl_3$) δ (ppm): 8.38-8.39 (d, 2H), 7.82-7.85 (m, 2H), 7.15-7.17 (d, 2H).

View Article Online
DOI: 10.1039/C4TC02631D

Synthesis of compound 3[12]

Tin powder (5.94 g, 50 mmol) was added in batches to a stirred solution of compound **2** (4.02 g, 10 mmol) in 48 mL ethanol and 30 mL 32% w/w aqueous HCl , then the mixture was heated to reflux for 2 hours. After cooling to room temperature, NaOH solution (2 mmol L^{-1}) was added until the solution was alkaline. Then, the resultant solution was extracted with dichloromethane, dried over anhydrous Na_2SO_4 and concentrated by rotary evaporation. The crude product was purified by column chromatography on silica gel using petroleum ether/tetrahydrofuran (v/v = 20/1) as eluent, a light brown solid was finally obtained in the yield of 85%. ^1H NMR (400 MHz, $CDCl_3$) δ (ppm): 6.94 (s, 6H), 3.75 (s, 4H).

Synthesis of compound 4[12]

Compound **3** (7.16 g, 20 mmol) and p-toluenesulfonic (17.18 g, 90.4 mmol) were dissolved in acetonitrile (200 mL) at 0 °C. After stirred for further 20 min, a solution of $NaNO_2$ (4.14 g, 60 mmol) and KI (12.45 g, 75 mmol) in water (40 mL) was added dropwise into it, the resultant mixture was warmed to room temperature and stirred overnight, then extracted several times with dichloromethane, dried over anhydrous Na_2SO_4 and concentrated by rotary evaporation. The crude product was purified by column chromatography on silica gel using pure petroleum ether as eluent, a white solid was finally obtained in the yield of 25%.

Synthesis of compound 5[13]

Compound **3** (1.8 g, 3.19 mmol) in anhydrous tetrahydrofuran (30 mL) was treated with n-BuLi (5 mL, 2.25 M in hexane, 11.25 mmol) at -78 °C for 30 min. After stirred at -78 °C for another 2 hours, dichlorodiphenylsilane (1.6 g, 6.38 mmol) was added dropwise into it, then the mixture was warmed to room temperature and stirred overnight. The solution was quenched with water and extracted several times with dichloromethane. The organic layer was dried over anhydrous Na_2SO_4 and concentrated by rotary evaporation. The crude product was purified by column chromatography on silica gel using petroleum ether/dichloromethane (v/v = 10/1) as eluent, a white solid was finally obtained in the yield of 35%. ^1H NMR (400 MHz, $CDCl_3$) δ (ppm): 7.83-7.84 (d, 2H), 7.70-7.72 (d, 2H), 7.58-7.62 (m, 6H), 7.40-7.46 (m, 2H), 7.36-7.38 (t, 4H).

Synthesis of compound 6

A mixture of compound **5** (1.02 g, 2.07 mmol), 4,4,4',4',5,5,5',5'-octamethyl-2,20-bi(1,3,2-dioxaborolane) (1.32 g, 5.19 mmol), potassium acetate (1.42 g, 14.49 mmol), and $Pd(dppf)_2Cl_2$ (150 mg, 0.2 mmol) in anaerobic 1,4-dioxane (45 mL) were refluxed under nitrogen for 12 h, and then water (20 mL) was added. The crude product was extracted with dichloromethane. The organic layer was dried over anhydrous Na_2SO_4 and concentrated by rotary evaporation. The crude product was purified by column chromatography on silica gel using petroleum ether/dichloromethane (v/v = 3/1) as eluent, a white solid was finally obtained in the yield of 65%. ^1H NMR (300 MHz, $CDCl_3$) δ (ppm): 8.20 (s, 2H), 7.93-7.94 (t, 4H), 7.64-7.67 (m, 4H), 7.34-7.40 (m, 6H), 1.35 (s, 24H).

Synthesis of Si-*p*TPE

Compound **6** (205 mg, 0.35 mmol), compound **7** (296 mg, 0.72 mmol), $Pd(PPh_3)_4$ (0.10 g, 0.08 mmol) and potassium carbonate (483 mg, 3.5 mmol) in 15 mL of tetrahydrofuran and 5 mL of distilled water were added into a 100 mL Schlenk tube. The resultant mixture was refluxed for 1 hour under nitrogen, then extracted with dichloromethane for several times. The combined organic extracts were dried over anhydrous Na_2SO_4 and concentrated by rotary evaporation. The crude product was purified by column chromatography on silica gel using petroleum ether/chloroform (v/v = 4/1) as eluent, a light green solid was finally obtained in the yield of 43%. ^1H NMR (300 MHz, $CDCl_3$) δ (ppm): 7.90-7.94 (d, 4H), 7.66-7.69 (d, 6H), 7.30-7.40 (m, 10H), 7.06-7.10 (m, 34H). ^{13}C (75 MHz, $CDCl_3$) δ (ppm): 147.8, 144.0, 143.1, 141.3, 140.1, 138.8, 137.0, 135.9, 132.7, 132.5, 132.1, 131.6, 130.5, 129.8, 128.4, 128.1, 127.9, 126.7, 126.3, 121.8. MS (MALDI TOF), (m/z): 994.4197 ($[M]^+$, calcd for $C_{76}H_{54}Si$, 994.3995. Anal. Calcd for $C_{76}H_{54}Si$: C, 91.71, H, 5.47. Found: C, 90.93, H, 5.59.

Synthesis of Si-tPE

Compound **6** (220 mg, 0.36 mmol), compound **8** (246 mg, 0.74 mmol), $Pd(PPh_3)_4$ (0.10 g, 0.08 mmol) and potassium carbonate (497 mg, 3.6 mmol) in 15 mL of tetrahydrofuran and 5 mL of distilled water were added into a 100 mL Schlenk tube. The resultant mixture was refluxed for 1 hour under nitrogen, then extracted with dichloromethane for several times. The combined organic extracts were dried over anhydrous Na_2SO_4 and concentrated by rotary evaporation. The crude product was purified by column chromatography on silica gel using petroleum ether/chloroform (v/v = 4/1) as eluent, a light green solid was finally obtained in the yield of 76%. ^1H NMR (300 MHz, $CDCl_3$) δ (ppm): 7.57-7.60 (d, 2H), 7.44 (s, 2H), 7.35-7.37 (d, 2H), 7.22 (s, 2H), 7.03-7.16 (m, 38H). ^{13}C (75 MHz, $CDCl_3$) δ (ppm): 146.9, 144.1, 144.0, 143.5, 141.2, 141.1, 137.4, 135.6, 135.4, 134.1, 133.2, 131.7, 129.9, 128.2, 128.0, 127.9, 126.7, 120.9. HRMS, (m/z): 842.3362 ($[M]^+$, calcd for $C_{64}H_{46}Si$, 842.3369. Anal. Calcd for $C_{64}H_{46}Si$: C, 91.17, H, 5.50. Found: C, 90.66, H, 5.80.

Synthesis of Si-*m*TPE

Compound **6** (205 mg, 0.35 mmol), compound **9** (296 mg, 0.72 mmol), $Pd(PPh_3)_4$ (0.10 g, 0.08 mmol) and potassium carbonate (483 mg, 3.5 mmol) in 15 mL of tetrahydrofuran and 5 mL of distilled water were added into a 100 mL Schlenk tube. The resultant mixture was refluxed for 1 hour under nitrogen, then extracted with dichloromethane for several times. The combined organic extracts were dried over anhydrous Na_2SO_4 and concentrated by rotary evaporation. The crude product was purified by column chromatography on silica gel using petroleum ether/chloroform (v/v = 4/1) as eluent, a white solid was finally obtained in the yield of 55%. ^1H NMR (300 MHz, $CDCl_3$) δ (ppm): 7.80-7.83 (d, 2H), 7.65-7.67 (d, 4H), 7.33-7.42 (m, 14H), 7.20-7.21 (d, 4H), 6.88-7.10 (m, 30H). ^{13}C (100 MHz, $CDCl_3$) δ (ppm): 146.3, 143.0, 142.7, 142.6,

View Article Online
DOI: 10.1039/C4TC02631D

142.5, 140.2, 139.8, 139.4, 139.0, 135.5, 134.7, 131.7, 131.5, 130.4, 130.3, 130.0, 129.2, 129.1, 128.5, 127.1, 127.0, 126.9, 126.7, 126.6, 125.6, 125.5, 125.4, 124.1, 120.3. HRMS, (m/z): 995.4075 ($[M+1]^+$, calcd for $C_{76}H_{55}Si$, 995.4073. Anal. Calcd for $C_{76}H_{54}Si$: C, 91.71, H, 5.47. Found: C, 91.59, H, 5.56.

Acknowledgements

We are grateful to the National Fundamental Key Research Program (2013CB834701), and the National Natural Science Foundation of China (no. 21161160556) for financial support.

Notes and references

[a] *Department of Chemistry, Hubei Key Lab on Organic and Polymeric Opto-Electronic Materials, Wuhan University, Wuhan 430072, China. Fax and Tel: 86-27-68755363; E-mail: lizhen@whu.edu.cn or lichemlab@163.com.*
[b] *Institute of Applied Chemistry, The Chinese Academy of Sciences Changchun 130022, China. E-mail: mdg1014@ciac.jl.cn.*
[c] *Key Laboratory of Organic Solids, Beijing National Laboratory forMolecular Science (BNLMS), Institute of Chemistry, Chinese Academy of Sciences, 100190 Beijing, China.*
[d] *Department of Chemistry, Beijing Normal University, Beijing, 100875, P. R. China.*

†Electronic Supplementary Information (ESI) available: DSC curves, AIE curves, CV plots, EL curves, NMR spectra for Si-pTPE, Si-tPE and Si-mTPE. See DOI: 10.1039/b000000x/

1 (a) J. Luo, Z. Xie, J. W. Y. Lam, L. Cheng, H. Chen, C. Qiu, H. S. Kwok, X. Zhan, Y. Liu, D. Zhu and B. Z. Tang, *Chem. Commun.*, 2001, 1740; (b) Y. Hong, J. W. Y. Lam and B. Z. Tang, *Chem. Soc. Rev.*, 2011, **40**, 5361; (c) Y. Hong, Jacky W. Y. Lam and B. Z. Tang, *Chem. Commun.*, 2009, 4332.

2 (a) B. Z. Tang, X. Zhan, G. Yu, P. P. S. Lee, Y. Liu and D. Zhu, *J. Mater. Chem.*, 2001, **11**, 2974; (b) H. Y. Chen, W. Y. Lam, J. D. Luo, Y. L. Ho, B. Z. Tang, D. B. Zhu, M. Wonga and H. S. Kwok, *Appl. Phys. Lett.*, 2002, **81**, 574; (c) G. Yu, S. Yin, Y. Liu, J. Chen, X. Xu, X. Sun, D. Ma, X. Zhan, Q. Peng, Z. Shuai, B. Z. Tang, D. Zhu, W. Fang and Y. Luo, *J. Am. Chem. Soc.*, 2005, **127**, 6335.

3 (a) Z. Zhao, Jacky W. Y. Lam and B. Z. Tang, *J. Mater. Chem.*, 2012, **22**, 23726; (b) L. Chen, Y. Jiang, H. Nie, P. Lu, H. H. Y. Sung, I. D. Williams, H. S. Kwok, F. Huang, A. Qin, Z. Zhao and B. Z. Tang, *Adv. Funct. Mater.*, 2014, **24**, 3621; (c) B. Chen, Y. Jiang, L. Chen, H. Nie, B. He, P. Lu, H. H. Y. Sung, I. D. Williams, H. S. Kwok, A. Qin, Z. Zhao and B. Z. Tang, *Chem. Eur. J.*, 2014, **20**, 1931.

4 (a) R. J. Tseng, R. C. Chiechi, F. Wudl and Y. Yang, *Appl. Phys. Lett.*, 2010, **88**, 093512; (b) K. T. Kamtekar, A. P. Monkman and M. R. Bryce, *Adv. Mater.*, 2010, **22**, 572.

5 Z. Zhao, S. Chen, Jacky W. Y. Lam, Cathy K. W. Jim, Carrie Y. K. Chan, Z Wang, P. Lu, C. Deng, H. S. Kwok, Y. Ma and B. Z. Tang, *J. Phys. Chem. C*, 2010, **114**, 7963.

6 (a) J. Huang, X. Yang, J. Wang, C. Zhong, L. Wang, J. Qin and Z. Li, *J. Mater. Chem.*, 2012, **22**, 2478; (b) J. Huang, N. Sun, Y. Dong, R Tang, P. Lu, P. Ca, Q. Li, D. Ma, J. Qin and Z. Li, *Adv. Funct. Mater.*, 2013, **23**, 2329.

7 (a) K. L. Chan, M. J. McKiernan, C. R. Towns and A. B. Holmes, *J. Am. Chem. Soc*., 2005, **127**, 7662; (b) R. Chen, Q. Fan, C. Zheng and W. Huang, *Org. Lett.*, 2006, **8**, 203; (c) H. Usta, G. Lu, A. Facchetti and T. J. Marks, *J. Am. Chem. Soc*., 2006, **128**, 9034; (d) C. W. Keyworth, K. L. Chan, J. G. Labram, T. D. Anthopoulos, S. E. Watkins, M. McKiernan, A. J. P. White, A. B. Holmes and C. K. Williams, *J. Mater. Chem.*, 2011, **21**, 11800.

8 D. Jana, B. K. Ghorai, *Tetrahedron*, 2012, **68**, 7309.

9 S. Kim, Y. Park, I. Kang and J. Park, *J. Mater. Chem.*, 2007, **17**, 4670.

10 W. Yuan, Y. Tan, Y. Gong, P. Lu, Jacky W. Y. Lam, X. Shen, C. Feng, H. Sung, Y. Lu, I. D. Williams, J. Sun, Y. Zhang and B. Z. Tang, *Adv. Mater.*, 2013, **25**, 2837.

11 S. Varughese, *J. Mater. Chem*. C., 2014, **2**, 3499.

12 E. Wang, L. Wang, L. Lan, J. Chen, J. Peng, Y. Cao, *Proc. of SPIE*, 2008, **7052**, 1.

13 K. Imai, Y. Kihara, A. Kimoto, J. Abe, Y. Tamai and N. Nemoto, *Polymer Journal*, 2011, **43**, 58.

View Article Online
DOI: 10.1039/C4TC02631D

New AIEgens containing tetraphenylethene and silole moieties: tunable intramolecular conjugation, aggregation-induced emission characteristics, and good device performance

Jie Yang, Ning Sun, Jing Huang, Qianqian Li, Qian Peng, Xi Tang, Yongqiang Dong, Dongge Ma* and Zhen Li*

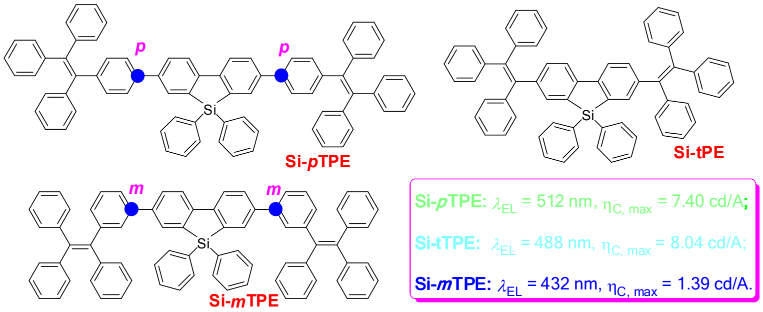

Si-*p*TPE: λ_{EL} = 512 nm, $\eta_{C,\ max}$ = 7.40 cd/A;

Si-tTPE: λ_{EL} = 488 nm, $\eta_{C,\ max}$ = 8.04 cd/A;

Si-*m*TPE: λ_{EL} = 432 nm, $\eta_{C,\ max}$ = 1.39 cd/A.

Three aggregation-induced emission (AIE) luminogens (Si-*p*TPE, Si-tPE and Si-*m*TPE) were successfully obtained by the covalent incorporation of tetraphenylethene to dibenzosilole core, their emission colors were tuned from green to sky blue even deep blue, through simple structural modification.